BEST AVAILABLE IMAGES

Defective images within this document are accurate representations of the original documents submitted by the applicant.

Defects in the images may include (but are not limited to):

- BLACK BORDERS
- TEXT CUT OFF AT TOP, BOTTOM OR SIDES
- FADED TEXT
- ILLEGIBLE TEXT
- SKEWED/SLANTED IMAGES
- COLORED PHOTOS
- BLACK OR VERY BLACK AND WHITE DARK PHOTOS
- GRAY SCALE DOCUMENTS

IMAGES ARE BEST AVAILABLE COPY.

As rescanning documents *will not* correct images, please do not report the images to the Image Problem Mailbox.

CONTAMINATION CONTROL
Series III – Contamination Control

SEMICONDUCTOR INTERNATIONAL®
The Industry's Source Book for Processing, Assembly & Testing

Design and Operation of UHP Low Vapor Pressure and Reactive Gas Delivery Systems

Suggestions on how to avoid contamination caused by condensation and corrosion in a reactive gas delivery system.

S. M. Fine
M.A. George
J. T. McGuire
Air Products and Chemicals, Inc., Allentown, Pa.

Key Technologies:

- Contamination Control
- Gas Delivery Systems
- Hydrogen bromide

At A Glance:

This paper describes gas handling methods and equipment design criteria required for consistent and reliable delivery of UHP low vapor pressure reactive gases. The effects of various atmospheric contaminants on the gas distribution system are investigated. A detailed study of the effect of moisture content on the corrosivity of HBr toward common materials of construction is presented as an example. The use of subatmospheric delivery pressure for low vapor pressure gases and methods for achieving stable flow to multiple usage points are also discussed. Fundamental models of heat transfer and fluid dynamics are used to show that substantial flow rates at low pressure can be maintained over large distances. Experimental results for WF_6 confirm the predictions of the models.

Consistent, reliable delivery of low vapor pressure reactive gases requires rigorous exclusion of atmospheric contaminants and careful control of system fluid dynamics. Gases such as HBr, SiH_2Cl_2, BCl_3 and WF_6 rapidly react with atmospheric H_2O to form gas-phase impurities or particles that contaminate the system. These impurities can adversely affect process performance and cause defects in the devices being fabricated.

Deposition of solid impurities can reduce the conductance, thereby increasing the pressure drop across the distribution system. Infiltration of atmospheric H_2O can lead to corrosion induced failures of gas handling components such as valves, regulators, mass flow controllers, and in some cases, corrosion-induced leaks in tubing and fittings.

Acid gases, such as HCl, HBr and HF, do not corrode many common materials of construction unless moisture is present.[1] The key to preventing corrosion in these systems involves removal of all the moisture from the system prior to introducing the acid gas and using ultrahigh purity process gas that does not reintroduce moisture into the system.

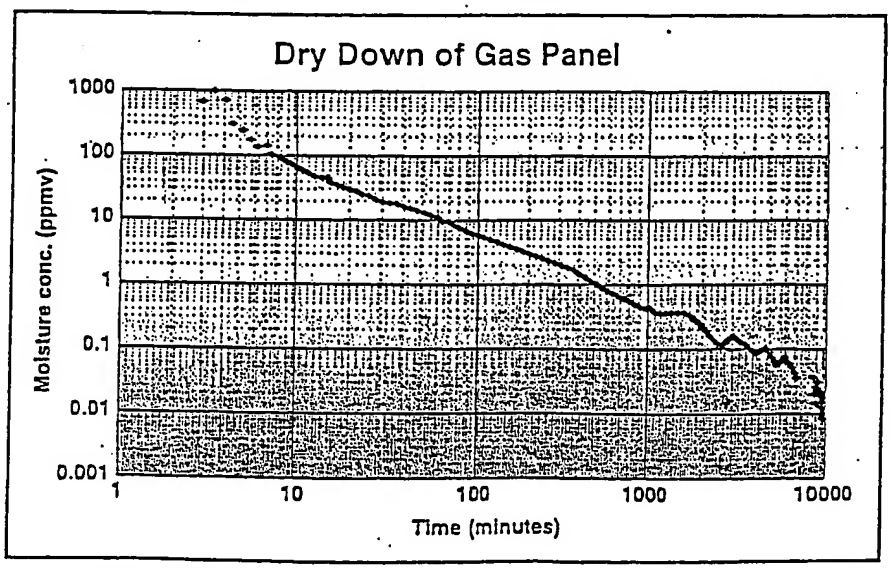

1. A process gas panel is dried down from 50% relative humidity at 70°F by flowing 200 sccm of purified nitrogen until the moisture level reaches the baseline level of the analyzer, about 10 ppb.

S.M. Fine, M.A. George, J. McGuire, "Design and Operation of UHP Low Vapor Pressure and Reactive Gas Delivery Systems", Semiconductor International, page 138, October 1995.

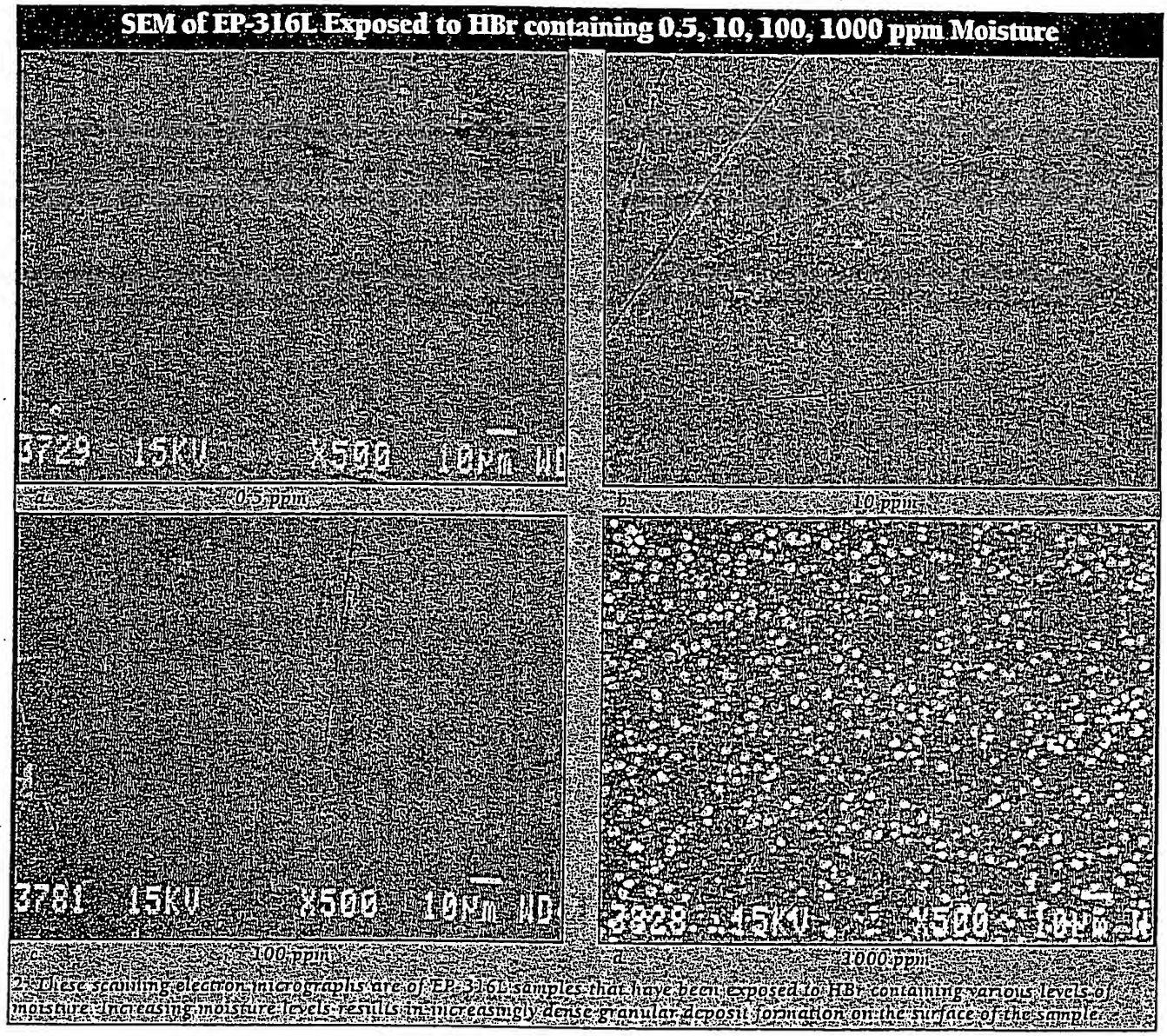

2. These scanning electron micrographs are of EP-316L samples that have been exposed to HBr containing various levels of moisture. Increasing moisture levels results in increasingly dense granular deposit formation on the surface of the sample.

In practice, most acid gases used in semiconductor fabrication are ultra-high purity and contain very little moisture. However, changing gas cylinders and replacing components on delivery systems requires opening these systems to ambient air, which has a moisture concentration up to 25,000 ppm. The intrusion of moisture into open acid gas systems is accelerated by the fact that these gases and the metal halide corrosion products they form are extremely hygroscopic. Thus, inadequate purging procedures after replacement of components or commissioning equipment are the main causes of failures in acid gas delivery systems used in the semiconductor industry.

Low vapor pressure gases such as WF_6, BCl_3, SiH_2Cl_2 and NH_3 can condense in an improperly designed or operated delivery system. Avoiding condensation requires operating the system at a temperature, pressure and flow rate that stays well below the saturated vapor pressure of the gas. The relative advantages to several approaches to solving this problem are discussed.

Moisture control

Moisture is often the critical contaminant in a gas distribution system. The intrusion of moisture into the gas distribution systems occurs primarily while changing gas cylinders or replacing components. Figure 1 shows the dry down of a process gas panel from 50% relative humidity at 70°F. The panel is dried down by flowing 200 sccm of purified nitrogen until the moisture level reaches the baseline level of the analyzer, about 10 ppb. The time required to fully dry down the panel is substantial. Incomplete removal of system moisture

0.5 mm on either side of the weld bead are attacked and strongly discolored.

At 1000 ppm moisture, a dense granular deposit and metal bromide particles (confirmed by EDS) cover most of the surface of the weld.

EP-HC22

The SEM data showed that HBr with 10-1000 ppm moisture does not cause any change in the surface morphology of this sample compared to an unexposed coupon.

At 10 ppm moisture, the EDS data shows no bromide incorporation into the surface of the electropolished Hastelloy C-22. However, the EDS spectrum at 1000 ppm moisture shows about 1 atom% bromide incorporation into the sample.

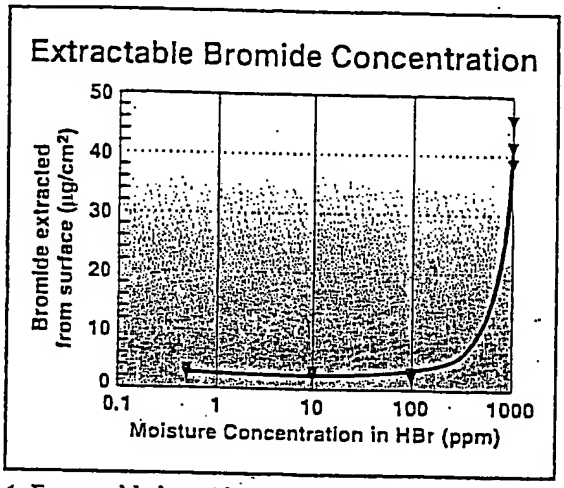

4. Extractable bromide concentration measured by IC as a function of moisture concentration during HBr exposure.

AFM results

Figures 3a-e show 1 × 1 µm AFM images of EP316L as received and exposed to HBr with various moisture levels. The control sample (Fig. 3a) exhibits a level of smoothness that is near the resolution of the instrument. The exposed samples (Figs. 3b-e) exhibit an increasing general roughening of the surface with increasing moisture content, with the HBr 1000 ppm moisture exposed sample being severally corroded compared to the other samples.

At 100 ppm moisture, the root mean squared amplitude of surface roughness, 70Å, is larger than the thickness of the surface oxide layer as measured by XPS sputter profile, a finding which is consistent with breakthrough of the surface oxide layer at this moisture concentration.

Ion chromatography (IC)

EP-316L as received and exposed to HBr containing the various moisture levels are analyzed by IC. The amount of bromide incorporated into the coupon as a function of the moisture level of the HBr exposure is shown in Fig. 4. The amount of bromide uptake into the coupon is independent of moisture concentration during the exposure for HBr with 0.5-100 ppm moisture, and about 10 times as much for HBr with 1000 ppm moisture. The bromide layer thickness of EP-316L exposed to HBr 0.5 ppm moisture is estimated as about 40Å using the IC data. This is consistent with a previous XPS study[10] and suggests that under ambient conditions, anhydrous HBr will brominate the surface oxide layer on EP-316L stainless steel.

Dew point data

The degree to which HBr attacks stainless steel is a function of the moisture concentration of the gas. The data above show that the surface of EP-316L stainless steel reacts with HBr containing as little as 10 ppm moisture. One might expect that general corrosion rates would increase dramatically at moisture levels high enough to form a liquid phase on the metal surface. How do these corrosion results relate to the dew point curve for the HBr/moisture system?

The dew point temperature (i.e., the temperature at which the mixture condenses) at 1 atmosphere total pressure for the HBr/moisture system has been measured at 0-20 ppm moisture[11] and above 1% moisture.[12] As the moisture concentration increases, the dew point of the HBr/moisture mixture increases and the saturated vapor pressure of the mixture decreases. Interpolation of the data suggests that the moisture concentration that gives a room temperature dew point at this pressure is about 300 ppm. At 1000 ppm moisture and 1 atmosphere HBr pressure, the mixture has a dew point well above room temperature and condenses concentrated aqueous hydrobromic acid on the surface of the coupons during the exposure.

The relative pressure of a system is defined as the partial pressure, P, divided by the saturated vapor pressure, P_o. If the relative pressure is less than 1, there is only a gas phase present. The dew point of a system (i.e., the point where a liquid phase begins to form) is defined to be when the partial pressure of the gas and its saturated vapor pressure at that temperature are equal. That is,

$$\frac{P}{P_o} = 1 \qquad [1]$$

At room temperature and 15 psia pressure of pure HBr, the relative pressure is:

$$\frac{P}{P_o} = \frac{15\ psia}{315\ psia} \qquad [2]$$

Addition of moisture reduces the saturated vapor pressure of HBr. At room temperature, 15 psia pressure and 300 ppm moisture, the saturated vapor pressure of HBr is reduced to 15 psia, and condensation occurs. However, the moisture concentration that results in a room temperature dew point is a function of the HBr pressure in the system. If the HBr pressure in the system were higher, less moisture would be required to give a condensed phase. The extreme case is on the high pressure side of a regulator attached to an HBr gas cylinder. The gaseous HBr is in equilibrium with a liquid filled cylinder and is therefore already at the saturated vapor pressure. Any residual moisture left in the system due to inadequate purging would be incorporated into a condensed phase on the surface of the delivery system.

We confirmed the effect of pressure on the extent of HBr induced corrosion of stainless steel. Samples of EP316L exposed to HBr (5 ppm moisture) at 315 psia show more attack by SEM and more bromide incorporation by IC and EDS than coupons exposed to HBr 1000 ppm moisture at 15 psia.

Delivery pressure

Consistent delivery of low vapor pressure gases requires preventing condensation of the gas in the process lines. Figure 5 shows the saturated vapor pressure versus temperature curve for WF_6. Condensation can be avoided by keeping the relative pressure (P/P_o) of WF_6 below one.

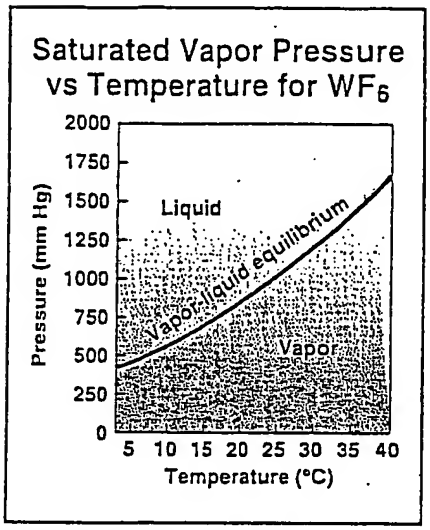

5. It's a good idea to keep the WF_6 partial pressure below half its room temperature saturated vapor pressure to accomodate changes in temperature of the delivery system.

However, the best practice is to keep the WF_6 partial pressure below half its room temperature saturated vapor pressure. This allows a reasonable safety margin to accommodate changes in temperature of the delivery system.

Maintaining a low relative pressure in the delivery system is typically achieved by one of three methods:

1. The cylinder and distribution system are heated. Typically, the cylinder is heated above 70°F and a positive temperature gradient is maintained to the point-of-use. This method requires a heating jacket for the cylinder and tubing heaters to the process tool. In some applications, heating may accelerate corrosion of the distribution system or cause decomposition of the process gas.
2. The cylinder is chilled to below the temperature of the coldest point in the distribution system. Special cylinder chillers are used to cool the cylinder.
3. The preferred method of avoiding condensation is to lower the delivery pressure of the gas. The delivery pressure of the process gas is maintained well below the saturated vapor pressure of the gas at the lowest temperature attained by the distribution system. Usually, an absolute pressure regulator is placed as close to the cylinder as possible and the vacuum system on the process tool is used to generate subatmospheric pressure in the distribution system.

Flow regimes

Typically, flow in process gas distribution systems is laminar. The maximum flow rate in this regime can be estimated using the equation[13] for compressible isothermal frictional flow:

$$F_{sccm} = \frac{60}{\rho} \cdot \frac{\pi D^2}{4} \cdot \sqrt{\frac{M.W.(p_a^2 - p_b^2) \cdot 1332^2}{2RT \ln \frac{p_a}{p_b} + \frac{f\Delta L}{2D}}} \quad [3]$$

Where

ρ = gas density at S.T.P.R = gas constant 83,070,979 (grams-cm-cc)/(cm²sec²mole K)
p_a = inlet pressure (Torr)
p_b = outlet pressure (Torr)
T = ambient temperature (K)
D = internal tube diameter (cm)
ΔL = length of pipe (cm)
f = fanning friction factor (dimensionless)
M.W. = molecular weight of gas in grams/mole

For 350 feet of 1/4 in. tubing, 280 Torr inlet pressure, 80 Torr exit pressure, a fanning friction factor of 0.01 (typical for EP stainless steel), and 25°C, Equation [3] predicts a maximum flow rate of 1.4 SLPM. This prediction agrees with experimental measurements of WF_6 flow through 350 foot lengths of 1/4 in. tubing at 298 K and 200 Torr pressure.[14]

The largest resistances to flow in a gas distribution system are the valves and pressure control devices. The maximum gas flow rate for a system can be modeled by combining the compressible gas flow equation and the valve configuration:

$$Fsccm = 8794.8 \cdot C_v \sqrt{\frac{\frac{p_a^2 - p_b^2}{\rho}}{7.17 \cdot 10^{-4}} \cdot T} \quad [4]$$

Where

C_v = flow coefficient for flow element (available from manufacturer)
ρ = density of gas in (grams/cc)
p_a = inlet pressure (Torr)
p_b = outlet pressure (Torr)
T = Temperature (K)
F_{sccm} = flow rate in (cc/min) at S.T.P.

For example, a 500 sccm flow of WF_6 gives a pressure drop of 5 Torr across a C_v = 0.08 valve at an inlet pressure of 280 Torr. While this is not a substantial pressure drop, the cumulative effect of many components is relatively large. Therefore, it is important to use the largest C_v components available. It also helps to reduce the amount of polymeric material in the flow path.

Polymers can contain large amounts of moisture that can react with process gases to form particles and/or swell the polymer.[15] WF_6 swells teflon valve seats, significantly reducing the C_v of the valve. This increases the pressure drop across the valve which can lead to Joule-Thompson cooling and condensation of the gas downstream of the valve.

Heat Transfer

The heat necessary to vaporize liquid from a liquid filled cylinder is transferred to the cylinder from the ambient. This heat load is described by equation [5]:

$$Q_{vap} = \Delta H_{vap} \cdot F \cdot \frac{\rho}{M.W.} \quad [5]$$

Where

Q_{vap} = heat transfer to cylinder (joules/min)
H_{vap} = heat of vaporization at cylinder conditions (joules/mole)
F = flow rate of gas (sccm)
ρ = density of gas (grams/cc)
M.W. = molecular weight of gas

If the heat transfer rate to the liquid remaining in the cylinder is not sufficient, the cylinder will cool and the cylinder pressure will drop. The heat transfer to a cylinder in a gas cabinet can be modeled using the correlation for heat transfer by natural convection (Equation [6]).[13] This assumes that heat transfer through the vertical walls of the cylinder is limited by the air-cylinder boundary layer and the heat transfer through the bottom of the cylinder is limited by the cylinder-liquid boundary layer (Fig. 6).

$$h = \frac{b \cdot k_f \cdot (N_{Gr} \cdot N_{Pr})^n}{D_o} \quad [6]$$

Where

k_f = thermal conductivity of air (0.0242 joules/(sec-m-K) @ 20°C)
D_o = diameter of cylinder (meters)
N_{Pr} = Prandtl number (0.69 @ 20°C)
N_{Gr} = Grashof Number
b = 0.54
n = 0.25

For a 9 in. diameter by 54 in. long cylinder, and a gas cabinet (2 ft × 2 ft) operating with 100 cfm air flow, the heat transfer coefficient is calculated to

be 2.9 joules/(sec-m²-K). The heat flux is calculated in the following manner:

$$Q = A \cdot h \cdot \Delta T \qquad [7]$$

Where
A = cross sectional area perpendicular to heat flux
ΔT = temperature difference between cylinder surface and fluid

For a 250 sccm flow of WF_6 (Hvap=25.7kJ/mole, gas density = 11.6 x10^{-03}g/cc), the heat load on the cylinder is calculated using equation [7] as 4.2 joules/sec. The maximum heat transfer through the cylinder walls increases linearly with the temperature difference between the ambient and the cylinder walls. Assuming ΔT = 2°C, the maximum available heat transfer rate to a cylinder is approximately 3.3 joules/sec, which is less than the heat load, 4.2 joules/sec. Therefore, the cylinder begins to cool as vapor is withdrawn. However, once ΔT becomes about 3°C, the heat transfer rate is approximately equal to the heat load by vaporization. The increasing ΔT, coupled with intermittent cylinder use, compensates for this heat drain and eventually allows a steady sub-ambient temperature to be obtained. Installation of a cylinder heater should be considered for constant high flow conditions.

Manifolding low vapor pressure gases

Semiconductor manufacturers have reduced the cost-of-ownership of gas delivery systems by manifolding one gas source to multiple usage points. While this is straightforward for high pressure gases, it can be problematic for low vapor pressure liquefied gases. Manifolding two or more independently operated mass flow controllers (MFCs) can cause flow control problems. The sudden increase in flow when a new MFC comes on line decreases the pressure in the delivery system (see equations [3] and [4] above). This causes the upstream pressure and flow rate on the other MFCs to oscillate until a new steady state pressure is reached. An absolute pressure regulator should be placed immediately upstream of each MFC to maintain a constant feed pressure and prevent flow oscillations when other process MFCs demand flow.

Conclusions

We have reviewed the effect of atmospheric moisture on corrosion of gas distribution systems, using HBr as an example. HBr corrosion of stainless steel is found to increase dramatically at the room temperature dew point concentration for moisture, about 300 ppm at 1 atmosphere HBr pressure. Below the room temperature dew point concentration, the amount of bromide uptake into stainless steel surfaces is small and relatively insensitive to the moisture concentration during the HBr exposure. HBr moisture compositions having dew points above room temperature result in extensive corrosion.

We have also discussed proper techniques for handling low pressure and reactive gases. We have shown the importance of methods and equipment that eliminate the intrusion of atmospheric H_2O and avoid condensation in the gas delivery system. A prototype WF_6 gas delivery system,[17] using these principles, has been operated in a fab environment with very favorable results.

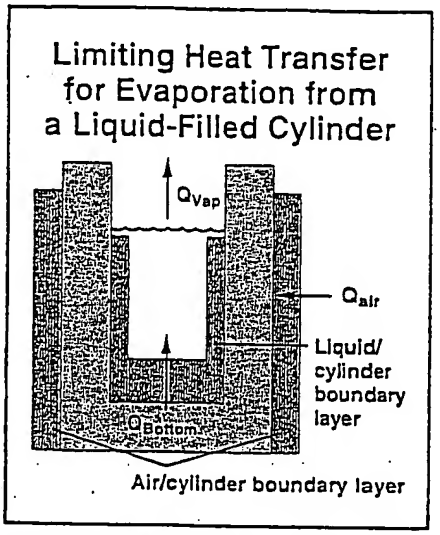

6. Limiting heat transfer to the cylinder requires the attainment of a constant temperature gradient between the liquid and the ambient.

Acknowledgments

The authors acknowledge Dave Bohling and Jack Hughes of Air Products for helpful discussions and Kent Harlan and Chris Magnella of Motorola for providing data on the WF_6 delivery system.

References

1. J. V. Martinez de Pinillos, P. J. Maroulis, and D. M. Drummer, in *Microcontamination 87 Conference Proceedings*, p. 89, Canon Communications, Santa Monica, CA (1987).
2. N. K. Verma, A. M. Haider, and F. Shadman, *J. Electrochem. Soc.*, 140, 1459 (1993).
3. B. K. Hennon and J. S. Overton, "UHP Stainless Process-Gas Piping System, Part II," *Microcontamination*, pp. 31, Canon Communications, Santa Monica, CA, March 1988.
4. G. H. Smudde, M. A. George, J. G. Langan, and W. I. Bailey, in *Microcontamination 92 Conference Proceedings*, p. 487, Canon Communications, Santa Monica, CA (1992).
5. T. A. Tabler, T. G. Wear, and W. Plante, in *Microcontamination 93 Conference Proceedings*, p. 422, Canon Communications, Santa Monica, CA (1993).
6. E. Ozawa, A. Boireau, H. Takagi, M. Miyazaki, H. Chevrel, T. Hattori, and J. Friedt, in *21st Symposium on ULSI Ultra Clean Technology Conference Proceedings*, p. 167, Tokyo, Japan (1994).
7. S. Takahashi, S. Miyoshi, T. Kojima, T. Koyama, and T. Ohmi, in *Microcontamination 93 Conference Proceedings*, p. 596, Canon Communications, Santa Monica, CA (1993).
8. S. M. Fine, R. M. Rynders, and J. R. Stets, *J. Electrochem. Soc.*, 142, 1286 (1995).
9. P. W. Atkins, Physical Chemistry, W. H. Freeman and Company, San Francisco (1982) p. 1065.
10. G. H. Smudde, personal communication.
11. Matheson Gas Products, SEMI Tech Brief (10/93).
12. H. Engels, Phase Equilibria and Phase Diagrams of Electrolytes, Chemistry Data Series, Vol. 9, Part 1, 102 (1990).
13. W. L. McCabe and J. C. Smith, "Unit Operations of Chemical Engineering," McGraw Hill, New York, 1976, and references therein.
14. M.A. George, U.S. Patent #5,137,047 (1992).
15. R.A. Hogle and P.C. Brown, in *Tungsten and Other Advanced Metals for ULSI Applications VI*, pp. 47-53, MRS, Pittsburgh PA, 1990.
16. R. Haney and M.A. George, in *Tungsten and Other Advanced Metals for ULSI Applicationss VI, Conference Proceedings*, pp. 63-70, MRS, Pittsburgh PA, 1990.
17. M. George, D. Bohling, W. Bailey, T Del Prato, K. Harlan, C. Magnella, *Semiconductor International*, p. 98, July 1993.

Additional Information
Air Products and Chemicals, Inc.
Electronics Division
7201 Hamilton Boulevard
Allentown, PA 18195-1501
Phone (610) 481-7519
Fax (610) 481-5361

Reprinted from SEMICONDUCTOR INTERNATIONAL October, 1995
Pub. No. 325-9613